

Flagellar Swimming for Medical Micro Robots: Theory, Experiments and Application

Gábor Kósa, Péter Jakab, Nobuhiko Hata, Ferenc Jólesz, Zipi Neubach, Moshe Shoham, Menashe Zaaroor and Gábor Székely

Abstract— Flagellar swimming is one of the swimming methods used by micro-organisms to advance in aquatic environment. The undulating motion of the flagella was successfully imitated to create propulsion for a medical swimming micro robot. The influence of a head section on the performance of such a robot is shown analytically. Swimming experiments demonstrate forward and backward swimming of a novel magnetically driven swimming tail. We intend to use the flagellar swimming tail in a three tail configuration for neurosurgical intervention in the ventricular system.

I. INTRODUCTION

THE late advances in smart pills [1] shows the advantage of an untethered device to reach previously inaccessible parts of the human body. Such a device can be a powerful diagnostic tool but it fully depends on the intestines peristaltic motion. In order to be able to do intervention or reach places where there is no natural driving force, one has to add self-propelling ability to the smart pill [2]. For example in the brain's ventricular system there are flows in the order of 1 [mm/s] (see [3]), but in contrary to the small intestines it will not insure that the smart pill will reach its target, thus positioning actuators are essential for the system.

Several studies suggested propelling mechanisms for medical robots using piezoelectric [4], ICPF [5] and magnetic [6-8] actuators.

Micro robots swim in low Reynolds number fluidic regime, for example a typical 0.1 mm micro robot that swims in water with a velocity of 1 mm/sec has a Reynolds number of 0.1. Due the reversibility in low Reynolds number flow (e.g. Stokes flow) the action of swimming micro organisms in nature are different from regular size swimmers such as fish [9]. All the micro swimming mechanisms such as

spermatozoa [10], cilia [11] and amoeba [12] create in one way or another a traveling wave, advancing in the opposite direction of the micro organism's locomotion. The simplest swimming method for a micro system is flagellar swimming by creating a planar or helical [13] traveling wave in an elastic tail. Fig. 1 compares between swimming of the spermatozoa of the lugworm *Arenicola marina* and the planar traveling wave created by a piezoelectric swimming tail [14].

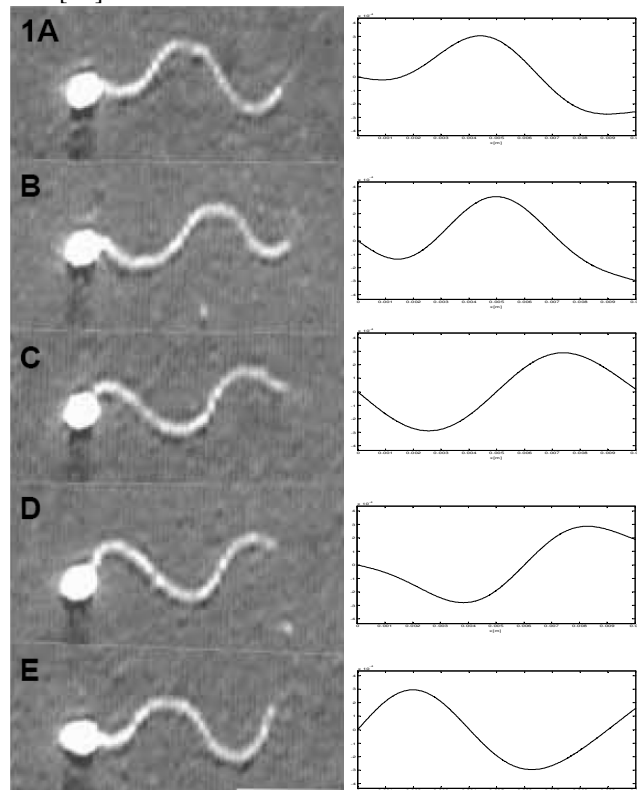


Fig. 1. Swimming action of a lugworm *Arenicola marina* spermatozoa [14] (left column) with the motion of the swimming tail based on 4 mode shape approximation (Right Column).

One can observe the similarity of the bending traveling wave to the spermatozoa's locomotion.

This paper presents in section II a theoretical model that calculates the influence of a head section on swimming, reports in section III on experimental results of swimming with a magnetic tail and introduces in section IV a robot design for a neurosurgical medical application.

Manuscript received March 15, 2008.

G. Kósa is with the Computer Vision Laboratory, Department of Information Technology and Electrical Engineering, ETH, Zurich, Switzerland (phone: 41-44-6327689; fax: 41-44-6321199; e-mail: gkosa@vision.ee.ethz.ch).

P. Jakab, N. Hata and F. Jólesz are with the Division of MRI and Image Guided Therapy Program at Department of Radiology, Brigham and Women's Hospital, Boston, MA and Harvard Medical School, Boston, MA, USA (e-mail: {Jakab, Jolesz}@bwh.harvard.edu)

Z. Yakov and M. Shoham are with the Faculty of Mechanical Engineering, Technion – Israel Institute of Technology, Haifa, Israel (e-mail: {zipiy, shoham@tx.technion.ac.il}).

M. Zaaroor is with the Department of Neurosurgery, Rambam Medical Center, Haifa, Israel (e-mail: m_zaaroor@rambam.health.gov.il).

G. Székely is with the Computer Vision Laboratory, Department of Information Technology and Electrical Engineering, ETH, Zurich, Switzerland (e-mail: szekely@vision.ee.ethz.ch).

II. THEORETICAL RESULTS

The swimming theory we developed was published in detail in previous publications. In this paper we present the influence of a head section on the swimming of a micro robot. For further details on swimming by creating a traveling wave in an elastic beam in viscous fluid see [4].

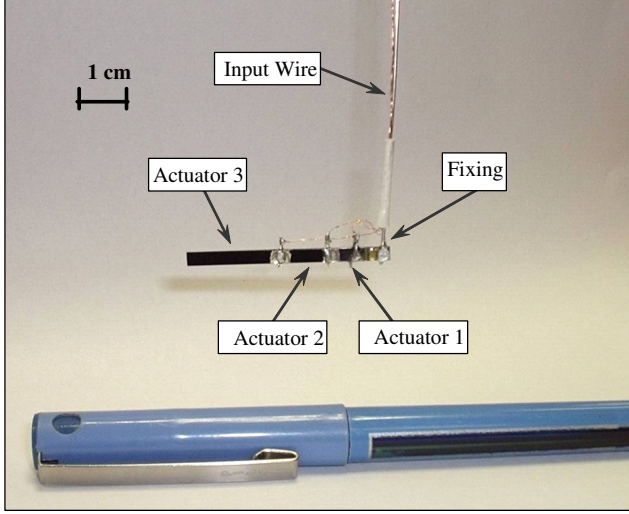


Fig. 2. A commercial piezoelectric bimorph (APC 40-1055) divided into three sections (Actuator 1-3) designed to create swimming.

A. Swimming tails

We are using two methods to create the propulsive force in the elastic beam:

1) **Piezoelectric bimorph bender** – This actuator uses a piezoelectric bimorph to create the traveling wave (see Fig. 2). The outer electrodes of the bimorph are divided into three sections, which are driven by three sinusoidal signals $\{V_1; V_2; V_3\}$ with the same frequency Ω and different amplitudes $\{G_1, G_2, G_3\}$ and phases $\{\Phi_1, \Phi_2, \Phi_3\}$.

2) **Magnetic coils** – a set of three coils are glued in series on a flexible printed board. Similarly to the previous method

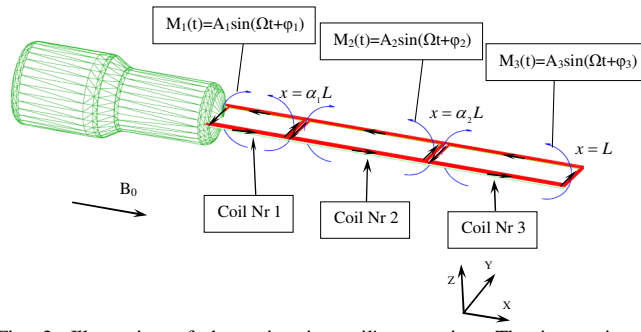


Fig. 3. Illustration of the swimming tail's operation. The interaction between the B_0 constant magnetic field in the x direction and three alternating currents in three coils, (the direction of the current in each coil is denoted by a black arrow) in the y direction creates alternating bending moments in the z direction. The moments have the same frequencies but different phases and amplitudes as shown.

the coils are driven by three signals. In the presence of a static magnetic field, B_0 , the Lorentz force:

$$F_{L_i}(t) = N_i b_i I_i(t) B_0 \quad (1)$$

where N_i is the number of turns in the i -th coil, b_i is the width of the coil and $I_i(t)$ is the current in the coil, creates a moment in each coil (see Fig. 3):

$$M_{L_i}(t) = l_i F_{L_i}(t) \quad (2)$$

The combination of the three moments creates a traveling wave along the tail.

B. The Heads Influence on Swimming

In a self propelled swimming body moving with constant velocity, the propulsive force is equal to the drag force of the body. The propulsive force of the swimming tail can be calculated from the drag force of a cylindrical rod. The explicit form of this force is [15]

$$F_p = \frac{2\pi\mu L U}{\ln(L/2\hat{c}_0) + 0.19315}, \quad (3)$$

where μ is the viscosity of the surrounding fluid, L is the length of the swimming tail, U is the velocity of the swimming tail and \hat{c}_0 is the first coefficient of the cross section shape function's Fourier decomposition

Assuming that the influence of the head on the flow around the swimming tail can be neglected, the reduction in the propulsive velocity of the micro robot due the addition of a head section can be calculated from the following equation:

$$F_H(U_R) + \frac{2\pi\mu L U_R}{\ln(L/2\hat{c}_0) + 0.19315} = \frac{2\pi\mu L U}{\ln(L/2\hat{c}_0) + 0.19315} \quad (4)$$

Where: $U_R^{(r)}$ is the reduced propulsive velocity and $F_H(U_R)$ is the drag of head of the micro robot. The drag force of the different head shapes is [17]:

$$F_H^{(s)}(U_R^{(s)}) = 6\pi\mu R_s U_R^{(s)}$$

$$F_H^{(d)}(U_R^{(d)}) = \frac{32}{3} \mu R_d U_R^{(d)} \quad (5)$$

$$F_H^{(r)}(U_R^{(r)}) = \frac{2\pi\mu L_r}{\ln(L_r/2R_r) + 0.19315} U_R^{(r)}$$

Where: $F_H^{(s)}(U^{(r)})$ is the drag force of a sphere with radius R_s , $F_H^{(d)}(U^{(r)})$ is the drag force of thin disc with radius R_d and $F_H^{(r)}(U^{(r)})$ is the drag force of a rod with length L_r and radius R_r .

The velocity reduction ratio between of the different head shapes is:

$$\frac{U_R^{(s)}}{U} = \frac{\eta}{3R_s + \eta}; \frac{U_R^{(d)}}{U} = \frac{\eta}{1.6976R_d + \eta}; \frac{U_R^{(r)}}{U} = \frac{\eta}{\eta_r + \eta} \quad (6)$$

Where:

$$\eta = \frac{L}{\ln(L/2A) + 0.19315}; \eta_r = \frac{L_r}{\ln(L_r/2R_r) + 0.19315}$$

Fig. 4 presents the reduction of the velocity for different volume ratios. The volume number is defined as ratio between the volume of the head and the volume of the swimming tail, Vol/LBT . In order to estimate the volume of disc we assumed that the disc thickness is fifth of its diameter, i.e. $t_d = 2R_d/5$. The same ratio was also assumed between the cylinders length and diameter, i.e. $L_r/2R_r = 5$.

Fig. 4 shows that the most efficient form is the flat disc

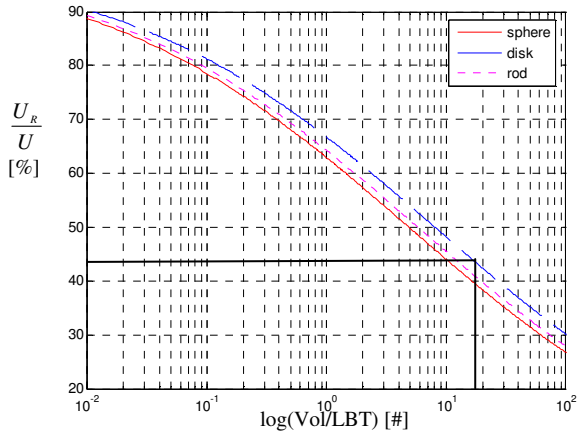


Fig. 4. Reduction of the velocity (%) due the addition of a head section with the shape of a sphere (solid red), a flat disc (blue dashed) and an elongated rod (magenta dotted) as a function of volume ratio (#). Our head design results in a velocity reduction of 43% (shown in black line) although the difference between this and the other shapes is less then 10%. The head reduces the propulsive velocity to 50% at volume number 12 i.e. when the head of the swimming micro robot is 12 times larger than the volume of the swimming tail.

A standard hearing aid battery, for example ZA 10 manufactured by Renata [16], has the following power capacity:

$$S_i = V_{nom} Ca_{nom} = 1.4[V] \cdot 95[mAh] / TP = 0.133 / TP, \quad (7)$$

where V_{nom} and Ca_{nom} are the nominal voltage and capacity of the battery, and TP is the operational time period in hours.

For an operational period of 1 [h] we need two ZA 10 batteries. The total volume of the batteries is $185[mm^3]$. Assuming that 20% of the head's volume is used for batteries, the head volume will be $925[mm^3]$. The volume of the swimming tail is $52.5[mm^3]$, thus the volume number is 17.62. Using the velocity reduction function for a flat disc (the most efficient packaging option), (6), this volume number will reduce the propulsive velocity by 43%.

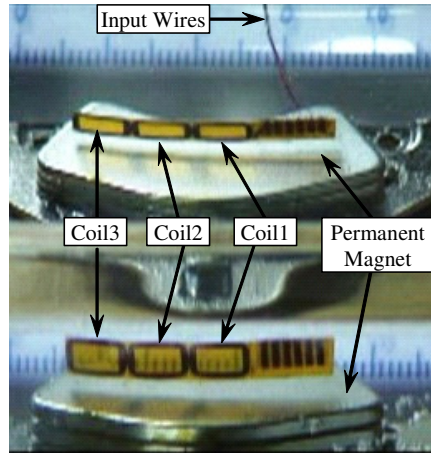


Fig. 5. Image of the experimental magnetic tail. The image shows the tail from two points of view: profile (lower image; reflection from the vessel wall) and half profile (upper image; direct image trough the water).

III. EXPERIMENTAL RESULTS

A. Setup and Methods

Previously we showed the swimming ability of piezoelectric swimming tail [4]. Using prior knowledge from these experiments, we built a magnetic coil tail and tested its swimming ability. Each coil had an outer length of 7 [mm] and height of 5 [mm] (see fig 5). The dimensions of the inner hole were 5×3 [mm] respectively. Each coil had 100 turns and was wound using copper magnet wire diameter of 0.02 mm. Three of such coils were mounted on a 0.05 [mm] thick foil. The total length of the tail was 21 [mm].

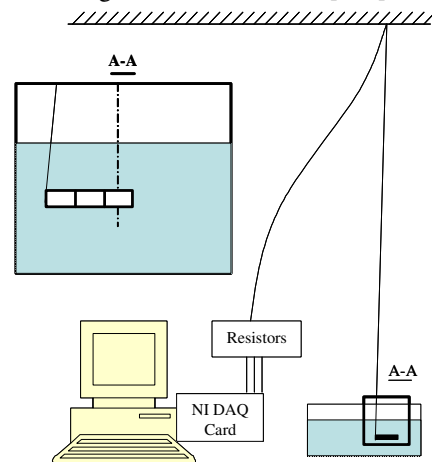


Fig. 6. Illustration of the setup of the swimming experiments.

The swimming tail was hung from the height of $l=1.72$ [m] over a hard disc's permanent magnet that produces a static magnetic field in parallel to the length of the swimming tail of about 0.2 [T]. The tail was driven by an NI PCIe-6259 DAQ card's D/A converter producing three signals with different phases and amplitudes. The currents of the input signals were set to:

$$\begin{aligned}
I_1 &= i_0 \sin 2\pi\Omega t \\
I_2 &= 2i_0 \cos 2\pi\Omega t, \\
I_3 &= -i_0 \sin 2\pi\Omega t
\end{aligned} \tag{8}$$

where $i_0 = 1.12[\text{mA}]$ designates is the signal amplitude and Ω is the frequency of the signals which has been varied between 10 and 125 [Hz] In order to achieve swimming backward we reversed the phases of the signals in (8).

Fig. 6 shows the scheme of the experimental setup. The weight of the tail was $m_2 = 0.073 [\text{g}]$ and the total weight of the wire was $m_1 = 0.29 [\text{g}]$.

From the deflection of the tail from its equilibrium point we can calculate the propulsive force:

$$F_p = \left(m_2 - \rho_o LBT + \frac{m_1}{2} \right) g \frac{\Delta}{l}, \tag{9}$$

where $\rho_o = 997[\text{kg}/\text{m}^3]$ is the density of the fluid (water), $g = 9.81[\text{m}/\text{s}^2]$ is gravity and Δ is the maximal distance the tail achieved.

Fig. 7 illustrates the swimming of the magnetic tail. The tail is driven with a frequency of $\Omega=25 [\text{Hz}]$ and amplitude of $i_i = 1.15 [\text{mA}]$. The image shows motion of the tail forward and backward.

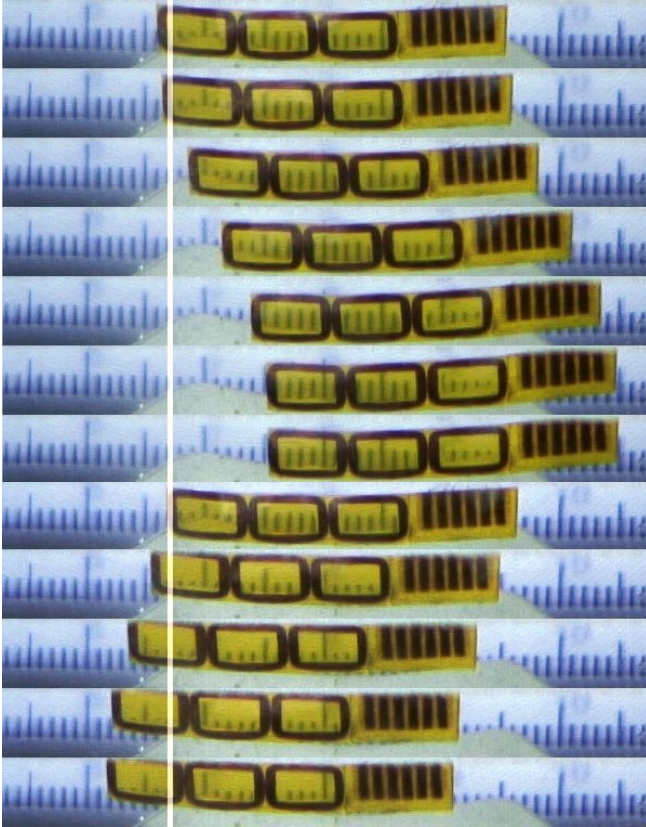


Fig. 7. Swimming of the magnetic tail forward (the upper 7 images) and backward (the lower 5 images). The vertical white line denotes the initial location of the tail.

In this experiment the swimming tail moved 9 [mm] forward and 5 [mm] back which are equivalent to a propulsive force of 10.3 [μN] and 5.7 [μN] accordingly.

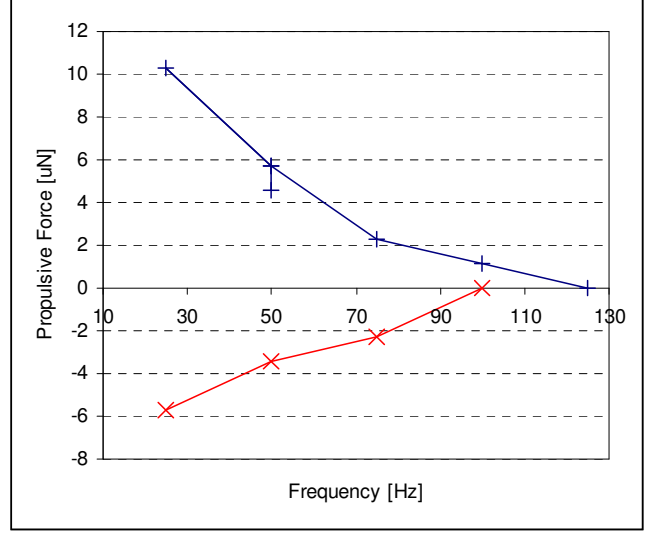


Fig. 8. Propulsive force versus frequency in forward (blue line with plus markers) and backward (red line with x markers) swimming of the magnetic swimming tail.

The magnetic swimming tail was tested in several frequencies from 1 to 150 [Hz]. Fig. 8 summarizes the results of those experiments. The lower the frequency the larger the propulsive force. The first natural frequency of the tail was found at $\omega_n=110 [\text{Hz}]$, we did not found any change in the decay of the swimming velocity at this frequency. When the phase difference between the coils is zeroed there is no propulsion. This result emphasizes the importance of undulating motion in small dimensions.

The Re number for the experiments is about 300 which is clearly a laminar flow, thus we will present in the future a proper swimming model based on earlier works on swimming of small fishes.

IV. MEDICAL APPLICATION

A flagellar swimming tail can be utilized for a large variety of bio-medical tasks. These medical applications include:

- 1) Examination of the gastrointestinal tract, including inspection of and intervention in the: esophagus, stomach, small intestine, colon and rectum [1].
- 2) Brain or spine inspection or surgery through the cerebrospinal fluid [4].
- 3) Thoracoscopy using a fluid to fill the chest cavity.
- 4) Kidney stone destruction [17].
- 5) Eye surgery [7].
- 6) Fetal surgery [18].

In general, flagellar swimming may fit any bio-medical application in which a robot advances in fluidic media. It can be proven that reducing the space in which micro-robot advances increases the efficiency of its swimming.

It has to be noted that flagellar swimming can hardly be useful for cardiovascular applications because of the fast velocities of the blood stream.

A. Swimming micro robot for brain surgery

One of the applications of a flagellar swimmer is interventions in the ventricular system in the brain.

Anatomically both the brain and the spinal cord (CNS, Central Nervous System) are immersed in transparent fluid similar to water, known as the CSF (Cerebrospinal fluid). The CSF is produced in the ventricles of the brain and flows out of the ventricular system to the subarachnoid space (SAS). This space covers both the brain and the spinal cord and connecting the internal cavities of the brain with the outer surface of the CNS. Theoretically, this space can be a conduit for introducing imaging and interventional devices that can reach pathologies without the need for conventional operative methods

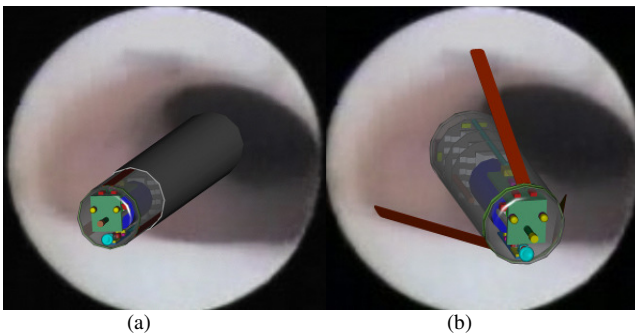


Fig. 9. Illustration of the swimming micro robot a) inserted by a cannula into the lateral ventricle and b) swimming to its target area. The background has been generated from an endoscopic image of the lateral ventricles.

There is a genuine need to explore these pathologies by minimally invasive methods for diagnosis, biopsies and ultimately for surgery. Ventriculosctomy is well established for treating lateral and third ventricle pathologies using mostly a rigid endoscope. Such a device has many limitations in the soft environment of the CNS. Currently, endoscopes are introduced trough a cannula into the lateral ventricles. When using rigid endoscopes, an opening of a diameter of $\text{\O}10$ [mm] in the brain is necessary in order to reach the target area. Since the surgeon wants to minimize damage to the brain, he needs to insert the endoscope as close as possible to the surgical target. Such a minimal distance approach, however, can endanger other parts in the brain and may damage them.

Flexible endoscopes are partially solving the problem but they still offer only limited access due to external tethering. We propose to use a swimming micro robot (although the robot itself will be about $1\text{-}2$ [cm^3] in size, its components will have to be produced by micro technologies) to perform the intervention. The device can be inserted through a cannula crossing a (potentially remote) functionally blank brain area but still could reach its target area without any strong spatial constraints.

We suggest the following interventional protocol for the robot:

- 1) Inserting a 6.6mm diameter cannula into the lateral

ventricle trough the right-frontal or right-parieto-occipital bone without jeopardizing functionally vital areas (standard procedure for ventriculostomy);

- 2) Introducing the robot trough the cannula into the lateral ventricle;

- 3) Navigation in the ventricle to reach the target area;

4) Inspection of the target area by high resolution imaging and local investigation of the electrical neuronal activity by the robot's built-in electrodes.

5) Targeted intervention: force guided biopsy, local chemotherapy or placement of radioactive agents for brachytherapy. If sufficient power is available, ablation or cauterization can also be carried out.

6.) Returning of the robot to the insertion point, and docking to the cannula.

- 7) Retrieving the robot and the cannula.

Fig. 9 illustrates the introduction of the swimming robot into the ventricular space.

The critical components in the robot are the following (See fig. 10):

1) Three flagellar swimming tails that pop out of the robot's body after introduction into the ventricle. The propulsion enables swimming in 5 degrees of freedom.

2) Power source made of batteries or magnetic coils for RF induction.

3) Custom designed IC for command, control and communication.

The payload for the robot will include:

- 1) Endoscopic camera [19] and LEDs.

2) Force sensor array to transmit tactile information and to increase the safety (warning of collision with the ventricle walls).

- 3) A magnetic tracking sensor for localization [20].

4) Micro tools for biopsy, and holding and deploying radioactive agents for brachytherapy.

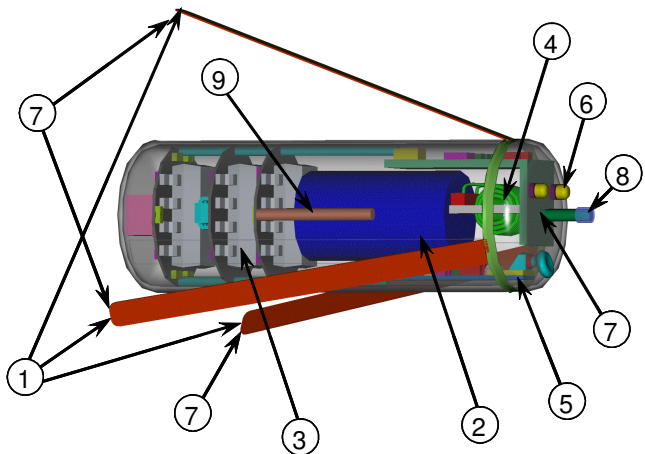


Fig. 10. Conceptual assembly of a swimming micro robot for neurosurgery. The components of the robot are: 1) Three swimming tails, 2) Power source (here 5 Renata ZA10 batteries in series), 3) Packaged IC for command control and communication, 4) Antenna, 5) Endoscopic Camera, 6) LEDs, 7) Force sensors, 8) Tool for intervention, 9) Localization sensor (here an Aurora magnetic tracker receiving coil).

This swimming robot has a diameter of $\text{Ø}6.6$ [mm] (determined mostly by the diameter of the batteries) and a length of 31 [mm] which results in a net volume of $1.1\text{ [cm}^3\text{]}$. The propulsive units' angle with the axis of the body is 30° and the outer diameter of the robot with open swimming tails is $\text{Ø}26$ [mm].

Such a robot will be able to swim with a velocity of about 1 [mm/s] in its axial direction. As it was shown earlier, for an operating period of 1 [hr], one hearing aid battery is necessary. The remaining batteries will be used mainly for powering the LEDs and the camera which are the main power consumers (the power consumption of the rest of the components can be neglected). The communication will be able to transmit to a distance of about 0.5 [m] and will operate bidirectionally.

V. CONCLUSION

In this paper we present new theoretical and experimental results towards utilizing flagellar swimming for medical application. To the best of our knowledge this is the first time demonstrating bi-directional swimming experimentally for planar wave propulsion. The theoretical results enable calculating the swimming properties of a combination of swimming tails and a head section. In addition, we propose a clinical procedure which can use flagellar swimming for propulsion and steering.

In the future we intend to realize the swimming robot described in section III for ventriculostomy and present a model that explains the experimental results presented in this work.

ACKNOWLEDGMENT

We would like to thank Prof. Matthew Bentley for the images of the swimming of a lugworm *Arenicola marina* spermatozoa presented in Fig. 1.

This publication was made possible by Grant Number 5U41RR019703, 5P01CA067165, 1R01CA111288, 1R01CA124377 from NIH. This study was also in part supported by NSF 9731748, CIMIT, Intelligent Surgical Instruments Project of NEDO, Japan.

REFERENCES

- [1] G. Iddan, G. Meron, A. Glukhovsky, and P. Swain, "Wireless capsule endoscopy," *Nature*, vol. 405, pp. 417, May 2000.
- [2] T. Ebevors and G. Stemme (Chief editor M. Gad-El-Hak), *The MEMS handbook*, Chapter 28- Micro-robotics, CRC Press, 2002, pp. 28-1 – 28-42.
- [3] V. Kurtcuoglu, M. Soellinger, P. Summers, K. Boomsma, D. Poulikakos, P. Boesiger and Y. Ventikos, "Computational investigation of subject-specific cerebrospinal fluid flow in the third ventricle and aqueduct of Sylvius," *Journal of Biomechanics*, vol. 40, pp. 1235–1245, 2007.
- [4] G. Kósa, M. Shoham and M. Zaaroor., "Propulsion Method for Swimming Micro Robots", *IEEE Transaction on Robotics*, vol. 23, pp. 137-150, Jan. 2007.
- [5] S. Guo, Y., Okuda and, K. Asaka, "Hybrid type of underwater micro biped robot with walking and swimming motions", IEEE Conference

- on Robotics and Automation (ICRA'05), vol. 3, pp 1604-1609, April 2004.
- [6] R. Dreyfus, J. Baudry, M.L. Roper, M. Fermigier, H.A. Stone, and J. Bibette, "Microscopic artificial swimmers", *Nature*, vol. 437, pp. 862-865, October 2005.
- [7] K.B. Yesin, K. Vollmers, and B.J. Nelson, "Modeling and control of untethered biomicrobots in a fluidic environment using electromagnetic fields," *International Journal of Robotics Research*, vol. 25, pp. 527-536, May 2006.
- [8] D. J. Bell, S. Leutenegger, L. X. Dong, B. J. Nelson, "Flagella-like Propulsion for Microrobots Using a Magnetic Nanocoil and Rotating Electromagnetic Field", Proc. of the 2007 IEEE Int. Conf. on Robotics and Automation (ICRA), April 2007.
- [9] T.Y.T. Wu, C.J. Brokaw and C. Bremsen Edt, *Swimming and flying in nature*, New York: Plenum Press, 1975, pp.161-173.
- [10] C.J. Brokaw, "Simulating the effects of fluid viscosity on the behaviour of sperm flagella," *Mathematical Methods in the Applied Sciences*, vol. 24, pp. 1351-1365, 2001.
- [11] Y. Okada, S. Takeda, Y. Tanaka, J.C. Belmonte. and N. Hirokawa, "Mechanism of Nodal Flow: A Conserved Symmetry Breaking Event in Left-Right Axis Determination," *Cell*, vol. 121, pp. 633–644, 2005.
- [12] W. Alt and M. Dembo, "Cytoplasm dynamics and cell motion: two-phase flow models," *Mathematical Biosciences*, vol. 156, 207-228, Mar. 1999.
- [13] G.I Taylor, "The action of waving cylindrical tails in propelling microscopic organisms," *Proceedings of the Royal Society A*, pp. 225-239, 1952.
- [14] A.A. Pacey, J.C. Cosson and M.G. Bentley, "The acquisition of forward motility in the spermatozoa of the polychaete *Arenicola Marina*," *Journal of Experimental Biology*, vol. 195, pp. 259-280, 1994.
- [15] J. Happel and H. Brenner, "*Low Reynolds number hydrodynamics*," Kluwer Academic Publisher group, 1983.
- [16] "ZA10 Maratone, Technical Data Sheet", Commercial publication of Renata SA, CH-4452 Itingen/Switzerland, 2008.
- [17] J. Edd, S. Payen, B. Rubinsky; M.L. Stoller and M. Sitti, "Biomimetic propulsion for a swimming surgical micro-robot," IEEE/RSJ Intelligent Robotics and Systems Conference, vol. 3, pp. 2583 – 2588, October 2003.
- [18] M. Berris, and M Shoham, "Febotics - a marriage of fetal surgery and robotics", *Computer Aided Surgery*, vol. 11, pp. 175-180, July 2006.
- [19] <http://www.medigus.com/cameras.html>
- [20] "Aurora Specifications", Commercial publication, NDI, D-78315 Radolfzell, Germany.